A BISTABLE SILICON PHOTONIC MEMS PHASE SWITCH FOR NONVOLATILE PHOTONIC CIRCUITS

Pierre Edinger[1], Alain Yuji Takabayashi[2], Carlos Errando-Herranz[1], Umar Khan[3], Cleitus Antony[4], Giuseppe Talli[4], Peter Verheyen[5], Wim Bogaerts[3], Niels Quack[2], and Kristinn B. Gylfason[1]

[1]KTH Royal Institute of Technology, SWEDEN

[2]Ecole Polytechnique Fédérale de Lausanne, SWITZERLAND

[3]Ghent University, BELGIUM

[4] Tyndall National Institute, IRELAND

[5]IMEC, BELGIUM

ABSTRACT

Silicon photonic circuits are rapidly growing in complexity and spreading to new applications. However, programmable circuits consume much power and require active electrical interfaces. For the first time, we demonstrate a nonvolatile photonic MEMS π-phase switch using dual comb-drive actuation and adhesion forces, implemented in a silicon photonics foundry. Both nonvolatile states are low-loss, display low dispersion, could be cycled through over 100 times, and have retention times over 12 hours. We believe that the demonstrated nonvolatility combined with excellent optical performance can enable a new generation of programmable photonic chips that do not consume any electrical power once (re)configured.

KEYWORDS

Silicon photonics, photonic MEMS, nonvolatile photonics, MEMS latching, phase shifter.

INTRODUCTION

Photonic integrated circuits (PICs) have experienced significant growth in complexity and scale in the last decade. Already in use in high-end datacenters, photonic chips are now being introduced in many fields where electronic chips cannot perform all tasks efficiently, such as in machine learning or quantum computing. However, photonic chips still require lengthy and costly development, slowing down their development for such applications and limiting the number of actors in the field. Therefore, generic chips that can be reprogrammed are needed to accelerate the development of PICs into new fields, just as Field-Programmable-Gate-Arrays (FPGAs) brought electronics to the hands of any willing circuit designer [1].

Programmable PICs can be implemented with a repetition of phase shifter and switch blocks forming a mesh-like circuit, but such building blocks need to display excellent performance for large-scale circuit scaling. Current active photonic devices are typically tuned with locally integrated heaters that consume a lot of power (>mW/device). Electrostatic MEMS actuators show promise as a low-power alternative, only consuming power when changing the device state (nW/device) [2,3]. However, most reported photonic MEMS actuators still require active biasing to maintain their state, limiting their usage to active programmable PICs.

Reconfigurable PICs based on nonvolatile devices further reduce the barrier of entry into photonic circuits, as generic photonic chips could then be (re)used for passive applications where active electrical connections are not available, see Figure 1. In recent years, nonvolatility in silicon photonics has been demonstrated with phase-change materials and different methods for switching but reported demonstrations required integration of non-standard materials [4]. A two-state nonvolatile silicon photonic MEMS power switch has been demonstrated on SOI using a nano-latch mechanism but required a large footprint [5]. Nonvolatile NEMS electrical switches have also been reported using adhesion forces and two curved actuators, but not on a photonic platform [6].

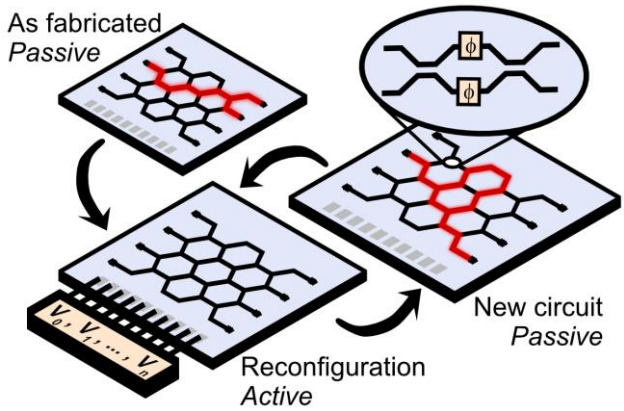

Figure 1: Nonvolatile photonic actuators could enable a new generation of programmable photonic circuits that can be (re)configured for different purposes and (re)used without consuming any electrical power.

Here, we experimentally demonstrate a photonic MEMS phase switch using adhesion forces and dual comb-drive actuators. Our switch can be set and reset to two nonvolatile states with a π-phase difference over 100 times, exhibits the lowest insertion loss of reported nonvolatile photonic devices, and can retain its states for more than 12 hours.

DEVICE DESIGN

Our nonvolatile photonic MEMS phase switch is composed of three main elements, see *Figure 2*. First, a suspended shuttle can be moved back and forth using opposing comb-drive actuators connected to independent biases. Second, the shuttle movement induces a phase shift along a suspended waveguide by modifying its modal cross-section, as a narrow silicon rib is moved

along with the shuttle. Third, the shuttle can be latched to mechanical stoppers with sufficient displacement in one direction and unlatched with sufficient bias on the opposing comb-drive actuator. Thus, the device can be switched between two nonvolatile states for the phase shift, corresponding to two different waveguide cross-sections, see inset in *Figure **2***.

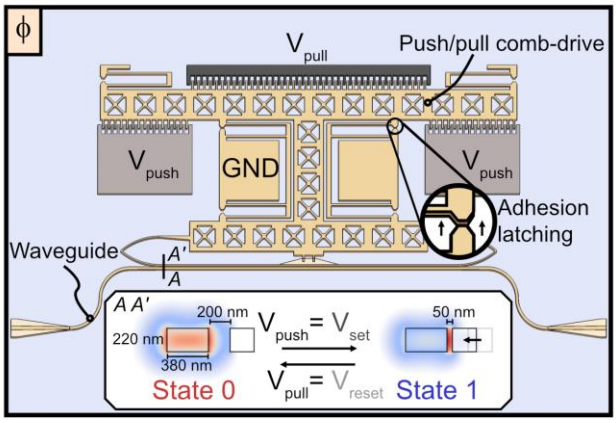

Figure 2: The design of our MEMS-based nonvolatile phase switch for programmable photonic circuits (to scale). A shuttle can be moved back and forth using opposing comb-drive actuators and latched to a new passive state using adhesion to mechanical stoppers, switching the phase in a suspended waveguide.

DEVICE IMPLEMENTATION

We implemented our device on a silicon photonics foundry platform, IMEC's iSiPP50G, see *Figure **3***. The platform includes a 220 nm thick SOI device layer for waveguides and passive photonic components and three metal layers for routing and electrical interfacing. Additionally, the implementation on the foundry platform allowed for doping the device layer in the MEMS comb-drives and included a back end of the line (BEOL) dielectric etching step to prepare for the release of the photonic MEMS devices. After foundry processing, we diced the 200 mm foundry wafers into chips and released the device using three main post-processing steps. First, we used a short buffered-HF step to clear the remaining 10 nm of planarization SiO_2 above the MEMS device. Second, we deposited and patterned a 50 nm-thick layer of Al_2O_3 to protect the BEOL. Third, we used vapor HF etching to remove the buried oxide layer (BOX) underneath the actuators. The final cross-section is shown as an inset in *Figure **3***. For more details on the post-processing steps, we refer readers to a previously published waveguide switch on the same platform [7].

We measured the change in phase and insertion loss versus actuation voltage by inserting the device in one arm of an integrated Mach-Zehnder Interferometer (MZI). We used grating couplers, waveguides, splitters, and bondpads from the foundry Process Design Kit (PDK) for optical/electrical interfacing and for the MZI circuit. For every voltage step, we measured the transmission through the MZI over multiple interference fringes and fitted the data to an MZI model to obtain phase shift and insertion loss [3].

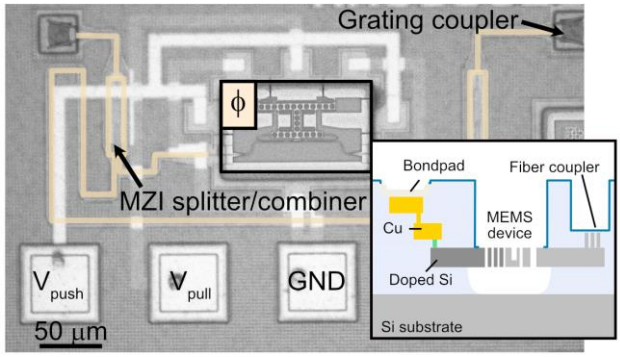

Figure 3: Microscope top view of our MEMS phase switch, implemented on IMEC's iSiPP50G silicon photonics foundry platform. Inset: cross-sectional sketch of the iSiPP50G platform with post-processed MEMS.

RESULTS AND DISCUSSIONS

We present the main operation cycle of our nonvolatile device in Figure 4(a). The phase shifter reaches more than 2π when increasing the bias V_{push}, corresponding to a reduction in the air gap between the waveguide and the tuning rib. If we increase V_{push} beyond 18 V, the phase shift does not increase any more, as contact with the mechanical stoppers limits the displacement. At that point, lowering V_{push} back to 0 V leaves the phase at a nonvolatile π offset. The device can then be reset to its original state by increasing the bias V_{pull} above a threshold voltage. The two different states display a difference of exactly π at a wavelength of 1570 nm, with a large extinction ratio of 37 dB, see Figure 4(b).

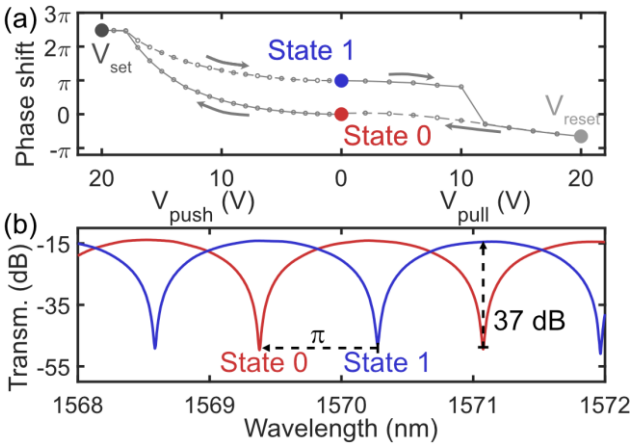

Figure 4: Optical characterization of our nonvolatile phase switch (a) Operation cycle: by setting bias V_{push} to 20V, the movable shuttle reaches and stays attached to the stoppers, resulting in a different passive state when lowering V_{push} back to 0V. The device can then be reset with $V_{pull} = V_{reset}$. (b) Transmission from 1568 to 1572 nm for both nonvolatile states.

We characterized the two optical states from 1500 to 1580 nm, see *Figure **5***. The difference in phase between both passive states shows a low dispersion of 0.005π/nm. Both states display very low insertion loss around 0.13 dB over the whole wavelength range.

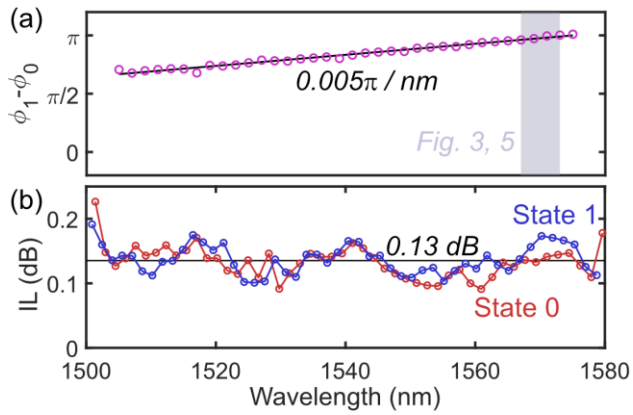

Figure 5: Optical characterization from 1500 to 1580 nm. (a) The device shows low and linear dispersion between the two nonvolatile states and (b) low, state-independent, and broadband insertion loss.

Finally, we verified that the device could be set/reset over 100 times without a noticeable performance decrease, see Figure 6(a). The latched state can be retained over 12 hours after disconnecting the electrical probes, see Figure 6(b). For the cycling tests, we chose both V_{set} and V_{reset} as 20 V. The biases were enough for the operation of the device over 100 cycles. However, we observed that the actual voltage required for release increased from 11±1 V to 19±1 V. The result suggests increased adhesion forces after repeated contact. While this could ultimately limit the number of cycles of the device, the actuator V_{pull} can be used up to 45V, which we expect to provide enough unlatching force for 1000s of cycles.

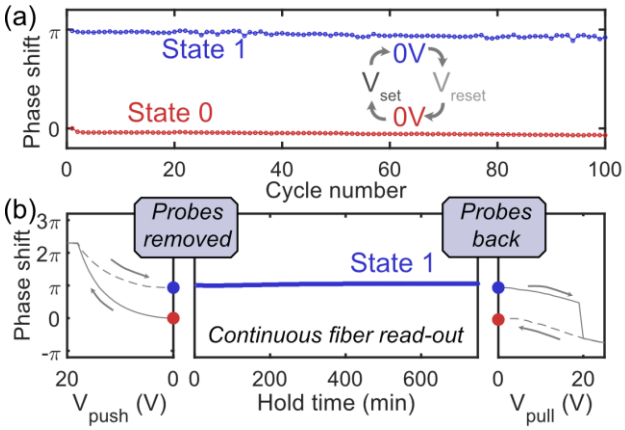

Figure 6: Device reliability measurements. (a) We cycled between the two nonvolatile states over 100 times and (b) measured a retention time of > 12 hours, both without a noticeable impact on the device performance.

CONCLUSION

In the present work, we have demonstrated nonvolatility on a silicon photonics platform using MEMS actuation. Our device can be set/reset between two optical phase states with comb-drive actuators and adhesion forces. We measured a phase difference of π between the passive and latched states at a wavelength of 1570 nm, which is required for full power switching in programmable interferometric circuits. The device displays low and broadband insertion loss, and small dispersion in the phase difference between the two nonvolatile states. Moreover, we verified that our nonvolatile phase switch can be set/reset over 100 times, and that it can retain its latched state over 12 hours after disconnecting electrical probes, both without subsequent loss in performance.

ACKNOWLEDGEMENTS

This work has received funding from the European Union's Horizon 2020 research and innovation programme under grant agreement No 780283 (MORPHIC). We thank Dr. Max Yan for access to measurement equipment and Mikael Bergqvist for assistance with setups.

REFERENCES

[1] W. Bogaerts *et al.*, "Programmable photonic circuits," *Nature*, vol. 586, pp. 207–216, Oct. 2020, doi: 10.1038/s41586-020-2764-0.

[2] C. Errando-Herranz, A. Y. Takabayashi, P. Edinger, H. Sattari, K. B. Gylfason, and N. Quack, "MEMS for Photonic Integrated Circuits," *IEEE J. Sel. Top. Quantum Electron.*, vol. 26, no. 2, pp. 1–16, Mar. 2020, doi: 10.1109/JSTQE.2019.2943384.

[3] P. Edinger *et al.*, "Silicon photonic microelectromechanical phase shifters for scalable programmable photonics," *Opt. Lett.*, vol. 46, no. 22, pp. 5671–5674, Nov. 2021, doi: 10.1364/OL.436288.

[4] Z. Fang, R. Chen, J. Zheng, and A. Majumdar, "Non-volatile reconfigurable silicon photonics based on phase-change materials," *IEEE J. Sel. Top. Quantum Electron.*, pp. 1–1, 2021, doi: 10.1109/JSTQE.2021.3120713.

[5] S. Abe and K. Hane, "Variable-Gap Silicon Photonic Waveguide Coupler Switch With a Nanolatch Mechanism," *IEEE Photonics Technol. Lett.*, vol. 25, no. 7, pp. 675–677, Apr. 2013, doi: 10.1109/LPT.2013.2248354.

[6] S. Rana *et al.*, "Nanoelectromechanical relay without pull-in instability for high-temperature non-volatile memory," *Nat. Commun.*, vol. 11, no. 1, Art. no. 1, Mar. 2020, doi: 10.1038/s41467-020-14872-2.

[7] A. Y. Takabayashi *et al.*, "Broadband Compact Single-Pole Double-Throw Silicon Photonic MEMS Switch," *J. Microelectromechanical Syst.*, pp. 1–8, 2021, doi: 10.1109/JMEMS.2021.3060182.

CONTACT

*P. Edinger, edinger@kth.se